ELSEVIER

International Journal of Mass Spectrometry 176 (1998) 245–252

Absolute total and partial electron impact ionization cross sections of hexamethyldisiloxane

R. Basner[a,*], R. Foest[a], M. Schmidt[a], K. Becker[b], H. Deutsch[c]

[a]*Institut für Niedertemperatur-Plasmaphysik, Robert-Blum-Str. 8-10, D-17489 Greifswald, Germany*
[b]*Department of Physics and Engineering Physics, Stevens Institute of Technology, Hoboken, NJ 07030, USA*
[c]*Institut für Physik, Ernst-Moritz-Arndt-Universität, Domstr. 10a, D-17489 Greifswald, Germany*

Received 26 February 1998; accepted 6 April 1998

Abstract

We studied the electron impact ionization of hexamethyldisiloxane (HMDSO), $Si_2O(CH_3)_6$, which is widely used in plasma-enhanced polymerization applications. Appearance energies and absolute partial cross sections for the formation of fragment ions with relative intensities >1% of the most abundant ion, the $Si_2O(CH_3)_5^+$ fragment ion, were measured in a high resolution double focusing sector field mass spectrometer with a modified ion extraction stage for electron energies from threshold to 100 eV. Dissociative ionization was found to be the dominant process. The main ionization channel removes a complete methyl group to produce the fragment ion $Si_2O(CH_3)_5^+$ with a cross section of 1.7×10^{-15} cm^2 at 70 eV. The stoichiometric and isotope composition of the various fragment ions was determined by using the high resolution ($m/\Delta m$ = 40,000) of the mass spectrometer used in these studies. The methyl ion is formed with considerable excess kinetic energy, whereas all other fragment ions are formed with essentially no excess energy. The experimental total single ionization cross section of HMDSO (2.2×10^{-15} cm^2 at 70 eV impact energy) is in good agreement with the result of a semiempirical calculation (2.1×10^{-15} cm^2 at the same energy). (Int J Mass Spectrom 176 (1998) 245–252) © 1998 Elsevier Science B.V.

Keywords: Hexamethyldisiloxane; Electron impact ionization; Cross sections; Plasma polymerization

1. Introduction

Low-temperature plasma technology is a rapidly growing field that plays a key role in many high-technology applications such as plasma-assisted thin film deposition, plasma etching, and surface treatment and cleaning [1]. The plasma-assisted polymerization is one of the most widely used thin film deposition techniques for surface protection and surface modification of optical devices, electronics components, and biomedical applications. Hexamethyldisiloxane (HMDSO), $(CH_3)_3$-Si-O-Si-$(CH_3)_3$, has been extensively used for the deposition of polymer layers on various substrates [2,3]. The electron-impact ionization of the monomer is one of the fundamental collision processes in a nonequilibrium, low-temperature plasma used in plasma deposition applications. The detailed understanding and the modeling of the plasma-enhanced deposition process require a knowledge of the total and partial electron-impact ionization cross sections. The shape of the cross section in the low-energy near-threshold region is particularly important for the properties of a low-temperature

* Corresponding author.

PII S1387-3806(98)14027-7

plasma, because this is the energy regime of maximum overlap between the ionization cross section and the energy distribution function of the plasma electrons [4]. Electron-impact induced ionization is not only the dominant process for the formation of charge carriers in the plasma, it is also the crucial step that initiates the multitude of plasma chemical reactions through the formation of reactive neutral and ionic radicals via dissociative ionization [4–8].

This paper presents the results of the mass spectrometric measurement of absolute partial and total electron-impact ionization cross sections of HMDSO, including all ions with relative intensities >1% of the most abundant ion, the $Si_2O(CH_3)_5^+$ fragment ion, from threshold to 100 eV. The measurements were carried out in a high-resolution double focusing sector field mass spectrometer with a modified ion extraction stage specifically designed for the reliable measurement of ionization cross sections. The high-resolution capability proved necessary for the identification of the various ion signals in terms of their stoichiometric and isotope composition. This study is part of our ongoing program to investigate ion formation processes in silane (SiH_4), the SiH_x (x = 1–3) free radicals, and various silicon-organic compounds such as tetramethylsilane (TMS), tetraethoxysilane (TEOS), and HMDSO. Preliminary results of the present study have already been published in Conference Proceedings [9]. The ionization of HMDSO was investigated earlier by Seefeldt et al. [10], but these authors limited their studies to the measurement of ionization cross sections for only four fragment ions and impact energies from threshold up to 50 eV.

2. Experimental

The experimental apparatus (Fig. 1) and the measurement technique employed here have been described in several previous publications [11–14]. Briefly, a modified, high-resolution ($m/\Delta m$ = 40,000) double focusing sector field mass spectrometer MCH 1310 with a Nier-type electron-impact ion source was used for the measurements. The electron gun was operated with a stabilized electron beam current of 10 μA, with an energy spread of ~0.5 eV (FWHM). The impact energy was varied from 5 to 100 eV. The electron beam is guided by a weak magnetic field (200 G). The target gas pressure in the ion source, which is typically in the range of 0.1–1 mPa compared with a background pressure of 0.001 mPa, was measured with a spinning rotor viscosity gauge. Argon, which is used as reference gas, was always added to HMDSO for calibration purposes. The ion efficiency curves (relative partial ionization cross sections) were measured simultaneously for Ar and the molecule under study in a well-defined mixture in an effort to ensure equal operating conditions for measurements of the fragment ions and the Ar^+ and Ar^{++} ions. The measured relative partial ionization cross sections were put on an absolute scale by normalization relative to the total Ar ionization cross section of 2.77×10^{-16} cm^2 at 70 eV [15]. Taking into account the uncertainties of ±7% from Rapp and Englander-Golden [15], the statistical uncertainty for our pressure measurement of ±3%, and for the ion signal of ±5%, the overall uncertainty in the absolute ionization cross sections reported here is about ±15%.

The reliability of the mass spectrometric technique for the measurement of parent and fragment ionization cross sections was demonstrated by Märk and coworkers [16–18]. These authors pointed out that discrimination effects and the loss of energetic fragment ions must be accounted for in order to obtain reliable dissociative ionization cross sections. Earlier measurements of the NF_3 and SO_2 parent and fragment ionization cross sections in our apparatus [11,12] demonstrated our ability to obtain reliable ionization cross sections for parent ions and fragment ions that are formed without excess kinetic energy, but revealed significant losses of energetic fragment ions. As a consequence, the ion optics for the extraction, acceleration, and deflection of the ions (Fig. 1) was rebuilt based on ion trajectory simulations [19] in conjunction with in situ experimental studies in an effort to minimize and/or quantify the discrimination of energetic fragment ions. The modified mass spectrometer can now be operated either in a high-mass resolution mode with significant discrimination ef-

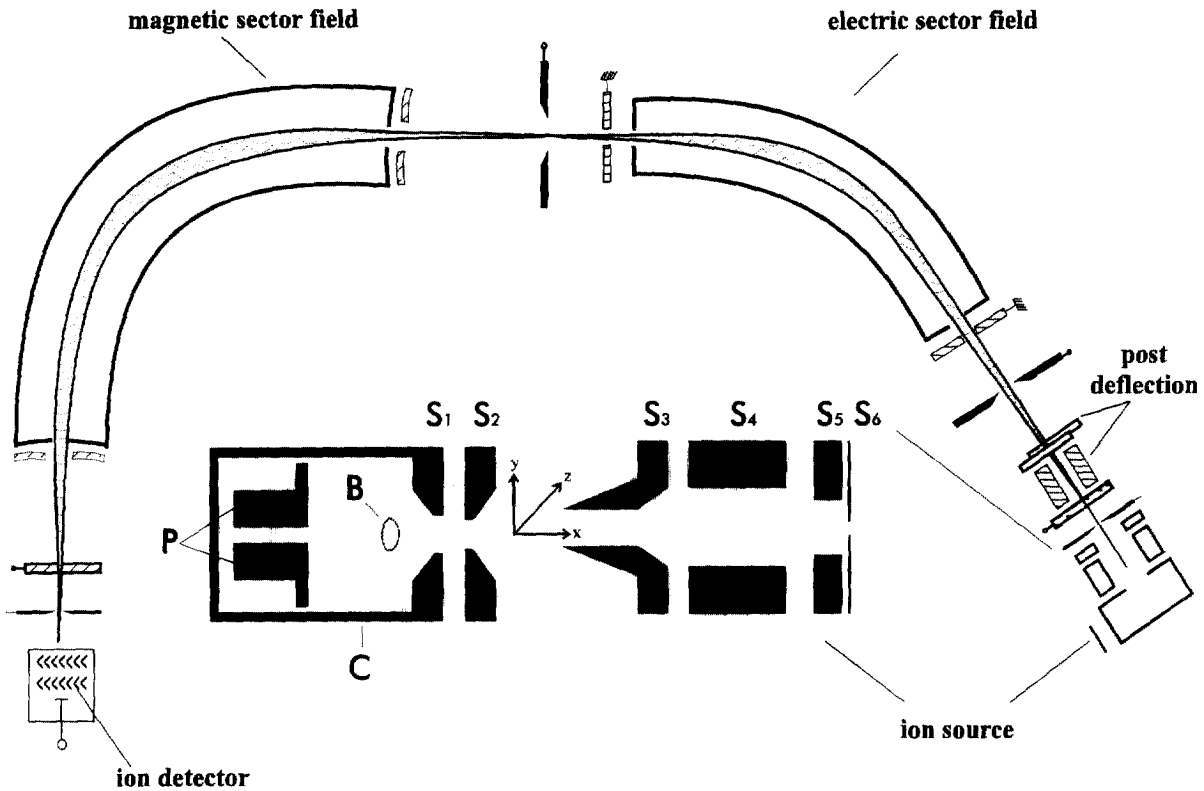

Fig. 1. Schematic diagram of the double focussing mass spectrometer system MCH1310 and a detailed view of the electron impact ion source used in the present study. *P*, pusher (5000 V); *C*, collision chamber (5000 V); *B*, electron beam (*z*-direction); S_1, collision chamber exit slit (5000 V); S_2, penetrating field extraction slit (5000–4580 V); S_3, ground slit (0 V); and S_4 and S_5, ion beam deflection electrodes (0–±1000 V).

fects for energetic fragment ions (corresponding to the following slit widths in Fig. 1: S_1 = 1 mm, S_2 = 1 mm, S_3 = 0.4 mm, $S_6 \leq 0.1$ mm) or in a high extraction efficiency mode by partially sacrificing the high mass resolution capability with a resulting mass resolution of 2000 (corresponding to slit widths in Fig. 1 of S_1 = 2.6 mm, S_2 = 2 mm, S_3 = 2.3 mm, S_4 = 3.6 mm, S_5 = 2 mm, $S_6 \leq 0.5$ mm). The calculated ion extraction efficiencies as a function of the excess kinetic energy were given and discussed by Basner et al. [20] for both modes of operation. Fig. 1 shows the configuration of the high extraction efficiency mode, which allows one to extract all ions with kinetic energy <3 eV to the entrance plane of slit S_4.

Märk and coworkers demonstrated [21–23] that the determination of reliable ionization cross sections for energetic fragment ions requires in general a sweep of the ion beam horizontally (*y*-direction in Fig. 1) and vertically (*z*-direction in Fig. 1) across the entrance slit of the mass spectrometer (S_6) and an integration of the ion signal over the measured two-dimensional beam profile. These authors also point out that the vertical sweep is important only for very energetic fragment ions and that reliable cross sections for less energetic fragment ions can be obtained by integrating over the horizontal beam profile alone. Our present experiment setup allows us to obtain horizontal ion beam profiles, but no vertical beam profiles. On the basis of our findings for the horizontal beam profiles obtained in this study for the various fragment ions from HMDSO, we expect that the only fragment ion for which a vertical integration could result in a noticeable change of the cross section is the CH_3^+ ion

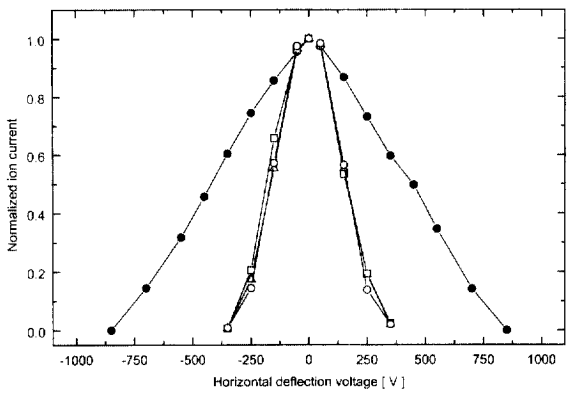

Fig. 2. Normalized ion beam currents of the ions m/z 147 ($Si_2OC_5H_{15}^+$) (open square), m/z 59 ($SiC_2H_7^+$) (open triangle), and m/z 15 (CH_3^+) (filled circle) from HMDSO and m/z 40 (Ar^+) (open circle) as a function of the horizontal deflection voltage of the extracted ion beam at 70 eV impact energy.

Table 1
Nominal masses (m/z), sum formulas (ion), measured appearance energies (AE), and measured relative intensities (70 eV) of HMDSO fragment ions, including the isotopes ^{28}Si, ^{16}O, ^{12}C, and ^{1}H

m/z	Ion	AE (eV)	Relative intensity (%)
162	$Si_2OC_6H_{18}^+$	8.8 ± 1.3	0.1
147	$Si_2OC_5H_{15}^+$	9.6 ± 0.5	100
133	$Si_2OC_4H_{13}^+$	14.8 ± 0.9	1.4
131	$Si_2OC_4H_{11}^+$	15.8 ± 0.7	3.8
73	$SiC_3H_9^+$	16.3 ± 0.6	9.3
73	Si_2OH^+	25.3 ± 1.5	1.6
66	$Si_2OC_4H_{12}^{++}$	26.8 ± 0.6	8.3
59	$SiC_2H_7^+$	22.0 ± 0.6	6.1
52	$Si_2OC_2H_8^{++}$	32.6 ± 0.8	1.8
45	$SiCH_5^+$	21.4 ± 0.7	5.5
45	$SiOH^+$	21.4 ± 1.4	0.7
43	$SiCH_3^+$	28.4 ± 0.7	2.4
15	CH_3^+	14.7 ± 0.8	2.6

for which we consequently only give a lower limit of its partial ionization cross section.

The horizontal ion beam profiles were obtained by sweeping the ion beam across the entrance slit of the mass spectrometer (S_6) in the y-direction with the help of the slits S_4 and S_5. The measured ion currents for a few selected ions (normalized to unity in their maxima to give the ion beam profiles) are shown in Fig. 2 as a function of the horizontal deflection voltage. Energetic fragment ions are identified by a broad ion beam profile in comparison with the ion beam profile of the Ar^+ ion, which has no excess kinetic energy. As a routine procedure in this work, we measured the ion beam profiles of all HMDSO fragment ions, as well as of the Ar^+ and Ar^{++} ions, at 70 eV impact energy under the condition of saturation of the ion current as a function of the extraction voltage (i.e. potential between S_1 and S_2). As an example, Fig. 2 shows our results for $Si_2OC_5H_{15}^+$, $SiC_2H_7^+$, and CH_3^+ from HMDSO and Ar^+. The only fragment ion found to be formed with significant excess kinetic energy is CH_3^+. Therefore, the absolute cross sections for the methyl ion were obtained by integrating the ion signal over the ion beam profiles of CH_3^+. Ion efficiency curves (relative ionization cross sections) for all other ions were measured at zero deflection voltage only, because this yields a signal that is representative of the complete ion beam because of the identical ion beam profiles (Fig. 2). The relative partial ionization cross sections as a function of the electron energy were measured in the high mass resolution mode to minimize the potential gradient in the ion source. We note that the mass spectral cracking patterns of the HMDSO/Ar mixture measured in our mass spectrometer at different electron energies (25, 50, 70, and 100 eV) in the high-resolution mode and in the high extraction efficiency mode were nearly identical at the same electron energy, which indicates that the various fragment ions are formed with little, if any, excess kinetic energy. The only exception to this is the peak at a mass-to-charge (m/z) ratio of 15 corresponding to the methyl ion, CH_3^+, where the peak height obtained in the high extraction efficiency mode was always higher (1.5 times at 70 eV) than the peak height measured in the high-resolution mode.

3. Results and discussion

The observed fragment ions of HMDSO are presented in Table 1, together with their respective appearance energies and relative intensities. The ions are listed in order of decreasing nominal mass. The results are given for the dominant isotope ^{28}Si

(92.3%). The much less abundant isotopes ^{29}Si (4.7%) and ^{30}Si (3.0%) give rise to two additional peaks at m/z 148 and 149, with relative intensities of 16% and 8%, respectively. The mass spectrum is essentially totally dominated by the fragment ion $Si_2OC_5H_{15}^+$ at m/z 147. No other fragment ion has a relative intensity of more than 10% of the $Si_2OC_5H_{15}^+$ signal. We note that there are two doubly charged fragment ions at nominal masses of 66 and 52 with appreciable intensities (Table 1). These results confirm previous observations [10] and are in accordance with the mass spectrum of HMDSO found in the tables of the NIST Mass Spectrometry Data Center [24]. However, in contrast to Seefeldt et al. [10] we assign the peak at m/z 66.5 to the isotope $^{29}Si_2OC_4H_{12}^{++}$ rather than to the $Si_2OC_4H_{13}^{++}$ ion based on the identical appearance energies, shapes of the ion efficiency curves, and expected relative intensities for the peaks at m/z 66, 66.5, and 67 of 8.3%, 1.2%, and 0.6%, respectively. The nominal masses 73 and 45 were found to exhibit a double-peak structure when using the high mass resolution of our instrument.

Measurements of the ion efficiency curves with special emphasis on the near-threshold region were carried out to determine the appearance energy of each fragment ion (Table 1). We used the linear extrapolation for the singly charged ions and the square root extrapolation method for the two doubly charged ions. For those four ions that were studied in this work as well as by Seefeldt et al. [10], our appearance energies are somewhat lower than the previously determined values. The quoted uncertainties in our measured values are due to the inherent energy spread of the electron beam and a small residual electrical field in the interaction region from the penetrating ion extraction field, which result in an extended curvature in the near-threshold region. We observed a much more extended curvature for the fragment ions compared with the onset of the ion efficiency curves of the rare gases Ar^+, Kr^+, Xe^+, and Xe^{++}, which were used for calibrating the electron energy scale (ionization energies: Radzig et al. [25]). We attribute this to the presence of different ionization channels and/or excitations of the ions. Fig. 3 shows the near-threshold data of m/z 40 (Ar^+) and

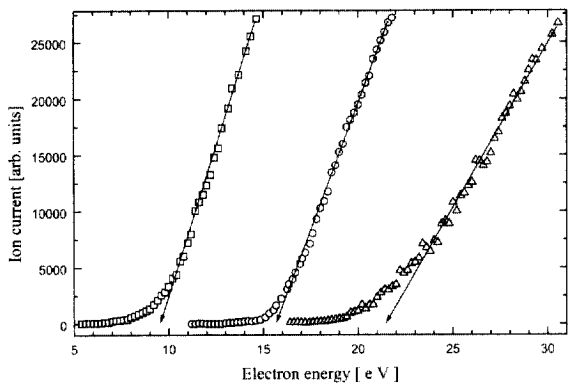

Fig. 3. Near-threshold data of the ions m/z 40 (Ar^+) (open circle), m/z 147 ($Si_2OC_5H_{15}^+$) (open square), and m/z 45 ($SiCH_5^+$) (open triangle).

the two fragment ions m/z 147 ($Si_2OC_5H_{15}^+$) and m/z 45 ($SiCH_5^+$), together with the linear extrapolation indicated by the arrows to demonstrate this behaviour and to understand the relevance of the determined appearance energies.

The absolute total and all measured partial electron impact ionization cross sections of HMDSO from threshold to 100 eV are presented in Table 2 and the corresponding graphs are shown in Figs. 4–6. The partial cross section for every silicon-containing fragment ion was obtained from the measured ion efficiency curves by adding the various isotope contributions. The molecular ion (m/z 162) shows an extremely small signal. A value of 0.1% of the m/z 147 base peak was determined for its relative intensity at 70 eV, which yields an absolute parent ionization cross section of $\sim 1.7 \times 10^{-18}$ cm^2.

As mentioned before, the fragment ions of HMDSO are formed with little, if any, excess kinetic energy. The only exception to this is the methyl fragment ion CH_3^+, which was found to be formed with appreciable excess kinetic energy. Similar findings were reported recently for the formation of the CH_3^+ fragment ion produced by dissociative ionization of tetramethylsilane [14]. Furthermore, the dominant ionization process for both silicon-organic compounds is the one in which a complete methyl group is removed. Integration of the horizontal CH_3^+ ion beam profile results in an ion signal that is 2.4 times

Table 2
Absolute partial and total electron impact ionization cross sections for HMDSO as a function of electron energy

Electron energy (eV)	Partial ionization cross section [10^{-16} cm^2] Ion											
	CH_3^+	$SiCH_3^+$	$SiCH_5^+$	$Si_2OC_2H_8^{+\,+}$	$SiC_2H_7^+$	$Si_2OC_4H_{12}^{+\,+}$	Si_2OH^+	$SiC_3H_9^+$	$Si_2OC_4H_{11}^+$	$Si_2OC_4H_{13}^+$	$Si_2OC_5H_{15}^+$	Total
9.8											0.16	0.16
10											0.28	0.28
11											0.94	0.94
12											1.70	1.70
13											2.78	2.78
14											4.42	4.42
15											6.60	6.60
16	0.011										7.33	7.34
17	0.015							0.012	0.021		9.30	9.35
18	0.021							0.028	0.027	0.015	10.8	10.89
19	0.027							0.055	0.039	0.028	12.1	12.25
20	0.034							0.088	0.054	0.039	13.2	13.42
21	0.037							0.12	0.099	0.063	14.7	15.02
22	0.042		0.014					0.19	0.16	0.086	15.5	15.99
23	0.053		0.027		0.017			0.27	0.22	0.12	16.0	16.71
24	0.058		0.039		0.031			0.36	0.31	0.15	16.2	17.15
25	0.064		0.049		0.058			0.48	0.41	0.18	16.3	17.54
26	0.078		0.069		0.070			0.59	0.56	0.21	16.4	17.98
28	0.093		0.14		0.18	0.027	0.014	0.79	0.67	0.24	16.5	18.68
30	0.12	0.015	0.19		0.28	0.071	0.020	0.97	0.74	0.27	16.6	19.35
35	0.14	0.044	0.39	0.024	0.55	0.37	0.042	1.30	0.86	0.30	16.6	21.00
40	0.15	0.096	0.54	0.066	0.72	0.68	0.072	1.47	0.85	0.29	16.6	22.28
45	0.15	0.15	0.62	0.13	0.81	0.96	0.11	1.49	0.78	0.28	16.6	23.17
50	0.15	0.22	0.69	0.19	0.85	1.18	0.15	1.49	0.74	0.26	16.6	23.89
60	0.23	0.32	0.80	0.28	0.92	1.40	0.21	1.46	0.68	0.25	16.6	24.83
70	0.35	0.38	0.84	0.31	0.96	1.49	0.26	1.42	0.64	0.24	16.7	25.39
80	0.50	0.43	0.89	0.34	0.96	1.55	0.29	1.38	0.60	0.24	16.8	25.87
90	0.64	0.47	0.90	0.39	0.96	1.62	0.32	1.31	0.58	0.24	16.8	26.24
100	0.79	0.48	0.90	0.39	0.97	1.65	0.33	1.24	0.58	0.24	16.8	26.41

larger than the ion signal obtained at zero deflection voltage. This has been taken into account in the quoted relative intensity of 2.6% for the CH_3^+ ion in Table 1. The shape of the CH_3^+ ionization cross section curve differs from all other cross section functions. The curve reaches a first plateau at an impact energy of ~40 eV and subsequently increases further and reaches a second plateau near 100 eV. This indicates that there are at least two channels leading to the formation of CH_3^+ ions, with a second, efficient channel opening up at ~50 eV (Fig. 4). As mentioned before, the CH_3^+ ion is the only HMDSO fragment ion where one might expect that a measurement of the vertical ion beam profile (which cannot be carried out in our apparatus) might lead to a further increase in the partial ionization cross section for this ion.

As one can see from Figs. 4–6, for most fragment ions the cross section increases with electron energy and reaches a plateau at ~80 eV. Only the cross sections corresponding to the ions with *m/z* 73 ($SiC_3H_9^+$), *m/z* 131 ($Si_2OC_4H_{11}^+$), and *m/z* 133 ($Si_2OC_4H_{13}^+$) show a maximum at lower energies between 30 and 50 eV. The previously reported cross section functions of Seefeldt et al. [10] for the ions with *m/z* 73 ($SiC_3H_9^+$), *m/z* 131 ($Si_2OC_4H_{11}^+$), and *m/z* 66 ($Si_2OC_4H_{12}^{+\,+}$), which are included in Fig. 5, show a shape up to the maximum energy investigated by these authors (50 eV), which is similar in shape to the present cross section curves, whereas for *m/z* 147

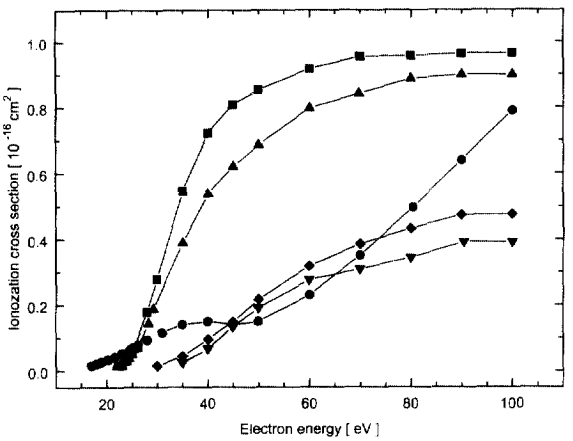

Fig. 4. Absolute partial HMDSO ionization cross sections of the fragment ions $SiC_2H_7^+$ (filled square), $SiCH_5^+$ (filled triangle), CH_3^+ (filled circle), $SiCH_3^+$ (filled diamond), and $Si_2OC_2H_8^{++}$ (filled inverted triangle) as a function of electron energy.

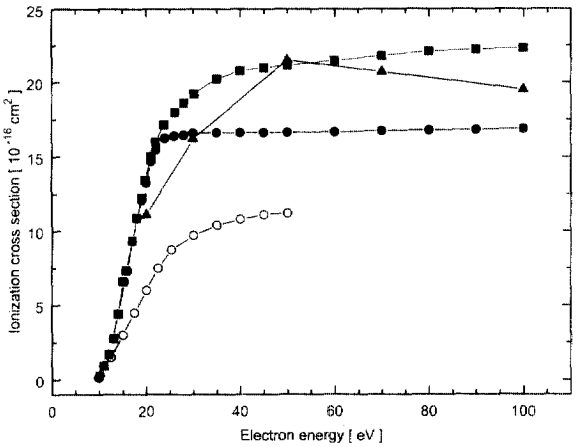

Fig. 6. Absolute total single HMDSO ionization cross section as a function of electron energy: the present results of measurement (filled square) and the calculated results (filled triangle) using the modified additivity rule [26,27]. Also shown are the absolute partial ionization cross section for the fragment ion $Si_2OC_5H_{15}^+$: present result (filled circle), previous result (open circle) of Seefeldt et al. [10].

$(Si_2OC_5H_{15}^+)$ the cross section shape measured in the present study is different (Fig. 6). Significant discrepancies exist between our absolute cross section values and the absolute data of Seefeldt et al. [10] for all four ions measured by these authors. Our cross sections are larger by factors ranging from 1.5 to 5.0. One possible explanation could be that Seefeldt et al. [10] had to rely on an indirect measurement of the gas pressure in their experiment, which was perhaps more susceptible to systematic errors.

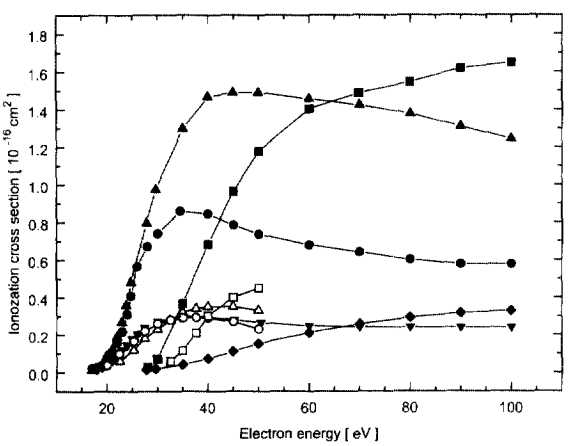

Fig. 5. Absolute partial ionization cross sections of HMDSO of the fragment ions $Si_2OC_4H_{12}^+$ (filled square, open square), $SiC_3H_9^+$ (filled triangle, open triangle), $Si_2OC_4H_{11}^+$ (filled circle, open circle), Si_2OH^+ (filled diamond), and $Si_2OC_4H_{13}^+$ (filled inverted triangle) as a function of electron energy. The full symbols represent present data; open symbols are the data of Seefeldt et al. [10].

The total HMDSO ionization cross section, listed in the last column of Table 2, is given as the charge weighted sum of all measured partial ionization cross sections. In Fig. 6 we show the total single ionization cross section, which is derived from the summation of the partial ionization cross sections of all singly charged ions. To our knowledge there are no other experimental determinations of this cross section. In the absence of rigorous theoretical methods that can be applied to the calculation of ionization cross sections for complex molecules, a semiempirical method was used for the calculation of the total single HMDSO ionization cross section. The modified additivity rule that was recently introduced by Deutsch et al. [26,27] incorporates weighting factors in an effort to account for molecular bonding. The application to the HMDSO molecule by using available cross sections for H [28], C [29], O [29], and Si [30], yields a calculated cross section that is somewhat below the experimental data over the entire energy range, with

the exception of the range around 50 eV (Fig. 6). The difference does not exceed 16% at any energy, which we consider a satisfactory agreement given the complexity of the target molecule.

4. Conclusions

We measured absolute partial cross sections for the electron impact ionization of the silicon-organic molecule HMDSO by using a mass spectrometric technique. Our relative ionization cross section measurements largely confirm the known mass spectral cracking pattern of HMDSO at 70 eV. We determined a complete set of appearance energies and absolute cross section values for the 13 most abundant ions produced by electron impact on HMDSO. Most fragment ions of HMDSO are formed with little, if any, excess kinetic energy, with the exception of the methyl ion for which the recorded ion beam profile indicated a significant amount of excess kinetic energy. The absolute values of the ionization cross sections measured here are indispensable for the modeling and understanding of plasma processes involving HMDSO and for the evaluation of mass spectrometric plasma diagnostics data.

Acknowledgements

One of us (K.B.) would like to acknowledge financial support for this project from the U.S. National Science Foundation (NSF) under grant PHY-9722438. The authors are grateful for the technical assistance provided by U. Haeder.

References

[1] M.A. Lieberman, A.J. Lichtenberg, Principles of Plasma Discharges and Materials Processing, Wiley, New York, 1994.
[2] A.M. Sarmadi, T.H. Ying, F. Denes, Eur. Polym. J. 31/9 (1995) 847.
[3] Y. Sawada, S. Ogawa, M. Kogoma, J. Phys. D. Appl. Phys. 28 (1995) 1661.
[4] K. Becker, V. Tarnovsky, Plasma Sources Sci. Technol. 4 (1995) 307.
[5] P. Kurunczi, A. Koharin, K. Becker, K. Martus, Contr. Plasma Phys. 36 (1996) 723.
[6] K. Becker, Comm. At. Mol. Phys. 30 (1994) 261.
[7] M. Schmidt, M. Maass, Contrib. Plasma Phys. 29 (1989) 197.
[8] R. Foest, M. Schmidt, M. Hannemann, R. Basner, in L.G. Christoph, D.R. James (Eds.), Gaseous Dielectrics VII, Plenum, New York, 1994, p. 335.
[9] R. Basner, R. Foest, M. Schmidt, K. Becker, Advances in Mass Spectrometry, Vol. 14, in press.
[10] R. Seefeldt, W. Möller, M. Schmidt, Z. Phys. Chem. 266 (1985) 797.
[11] V. Tarnovsky, A. Levin, K. Becker, R. Basner, M. Schmidt, Int. J. Mass Spectrom. Ion Processes 133 (1994) 175.
[12] R. Basner, M. Schmidt, V. Tarnovsky, A. Levin, K. Becker, J. Chem. Phys. 103 (1995) 211.
[13] R. Basner, M. Schmidt, H. Deutsch, Contrib. Plasma Phys. 35 (1995) 375.
[14] R. Basner, R. Foest, M. Schmidt, F. Sigeneger, P. Kurunczi, K. Becker, H. Deutsch, Int. J. Mass Spectrom. Ion Phys. 153 (1996) 65.
[15] D. Rapp, P. Englander-Golden, J. Chem. Phys. 43 (1965) 1464.
[16] K. Leiter, K. Stephan, E. Märk, T.D. Märk, Plasma Chem. Plasma Processes 4 (1984) 235.
[17] K. Stephan, H. Deutsch, T.D. Märk, J. Chem. Phys. 83 (1985) 5712.
[18] K. Leiter, P. Scheier, G. Walder, T.D. Märk, Int. J. Mass Spectrom. Ion Processes 87 (1989) 209.
[19] SIMION, Version 6.0, Idaho National Engineering Laboratory, EG&E Idaho Inc., Idaho Falls, ID, 1995.
[20] R. Basner, M. Schmidt, V. Tarnovsky, K. Becker, H. Deutsch, Int. J. Mass Spectrom. Ion Processes 171 (1997) 83.
[21] D. Margreiter, G. Walder, H. Deutsch, H.U. Poll, C. Winkler, K. Stephan, T.D. Märk, Int. J. Mass Spectrom. Ion Processes 100 (1990) 143.
[22] H.U. Poll, C. Winkler, D. Margreiter, V. Grill, T.D. Märk, Int. J. Mass Spectrom. Ion Processes 112 (1992) 1.
[23] V. Grill, G. Walder, D. Margreiter, T. Rauth, H.U. Poll, P. Scheier, T.D. Märk, Z. Phys. D 25 (1993) 217.
[24] NIST Mass Spectrometry Data Center, NIST Chemistry WebBook, EPA MS number 61595.
[25] A.A. Radzig, B.M. Smirnov, in J.P. Toennies (Ed.), Reference Data on Atoms, Molecules and Ions, Springer Series in Chemical Physics 31, Springer-Verlag, Berlin, 1985.
[26] H. Deutsch, T.D. Märk, V. Tarnovsky, K. Becker, C. Cornelissen, L. Cespiva, V. Bonacic-Koutecky, Int. J. Mass Spectrom. Ion Processes 137 (1994) 77.
[27] H. Deutsch, K. Becker, T.D. Märk, Int. J. Mass Spectrom. Ion Processes 167/168 (1997) 503. See also, R. Basner, K. Becker, H. Deutsch, M. Schmidt, Electron-impact ionization cross sections of si-organic compounds, in M. Inokuti, K. Becker (Eds.), Fundamentals of Plasma Chemistry, Academic Press, New York (1998) in press.
[28] W.L. Fite, R.T. Brackmann, Phys. Rev. 112 (1958) 1141.
[29] E. Brook, M.F.A. Harrison, A.C.H. Smith, J. Phys. B 11 (1978) 3115.
[30] R.S. Freund, R.C. Wetzel, R.J. Shul, T.R. Hayes, Phys. Rev. A 41 (1990) 3575.